Regular Article

PHYSICAL CHEMISTRY RESEARCH
Published by the
Iranian Chemical Society
www.physchemres.org
info@physchemres.org

***Phys. Chem. Res.**, Vol. 5, No. 3, 425-437, September 2017*
DOI: 10.22036/pcr.2017.67519.1323

Selective Binding of Cyclic Nanopeptide with Halides and Ion Pairs; a DFT-D3 Study

M. Khavani and M. Izadyar*

Department of Chemistry, Faculty of Sciences, Ferdowsi University of Mashhad, Mashhad, Iran

(Received 13 November 2016, Accepted 18 February 2017)

In this article, theoretical studies on the selective complexation of the halide ions (F^-, Cl^- and Br^-) and ion pairs (Na^+F^-, Na^+Cl^- and Na^+Br^-) with the cyclic nano-hexapeptide (CP) composed of L-proline have been performed in the gas phase. To calculate the dispersion interaction energies of the CP and ions, DFT-D3 calculations at the M05-2X-D3/6-31G(d) level were employed. Based on the results, F^- and Na^+F^- make the most stable complex with the CP. The dispersion interactions between the ions and the CP are small while the electrostatic interactions are a driving force for the complex formation. Finally, natural bond orbital (NBO) and quantum theory of atoms in molecules (QTAIM) analyses indicate that F^- makes the most stable complex with CP due to more charge transfer and stronger bond formation in comparison to other ions.

Keywords: Cyclic nanopeptide, Dispersion interaction, Ion pair, Selective binding, Halide

INTRODUCTION

Synthetic molecular receptors have important application in different fields such as ion recognition and biology [1-5]. The most important application of the molecular receptors is the selective complex formation in the solvent such as water [6-10]. Therefore, the designing of the selective receptors for the ion recognition in a highly competitive environment, is of interest for the chemists [11]. Generally, receptors can be broadly classified into two categories based on their structures as acyclic and cyclic receptors [12].

In acyclic receptors, the binding units are situated at the intervals along their length, whereas in the cyclic receptors the binding units are arranged around the close ring [13]. Cyclic receptors are macrocyclic compounds which are composed of the organic and bioorganic units which are more useful than acyclic receptors in the selective and stable complex formation with the ions and molecules [14].

Today, cyclic peptides (CPs) have gained increasing interest due to high ability in the eparation of the ions, organic and bioorganic molecules [15-17]. CPs are the new interesting compounds with many applications such as antimicrobial agents, ion channel, molecular receptor and bio-sensors [18-28]. They are able to make a stable channel in the lipid bilayer for ions and molecules transmission. For example, Ghadiri and co-workers synthesized a CP having the self-assembling ability in the cyclic peptide nanotube (CPNT) formation inside a lipid bilayer [29]. Also Granja research group synthesized a CP with aminocyclo-hexanecarboxylic acid units [30]. They investigated the ability of this CP in the CPNT formation inside the lipid bilayer by employing the experimental and theoretical methods. They showed that CPNT structure is able to transmit Na^+ ions across the lipid bilayer.

As mentioned, some CPs are able to form the selective complexes with the different ions and molecules. For example, Chermahini and co-workers by employing the theoretical calculations investigated the ability of some CPs composed of three and four amino acid units in the formation of the selective complexes with alkali metal ions [31,32]. Moreover, in our previous work by employing the DFT and molecular dynamic simulation methods we investigated the ability of some CPs composed of alanine, glycine and Valine amino acids in the

*Corresponding author. E-mail: izadyar@um.ac.ir

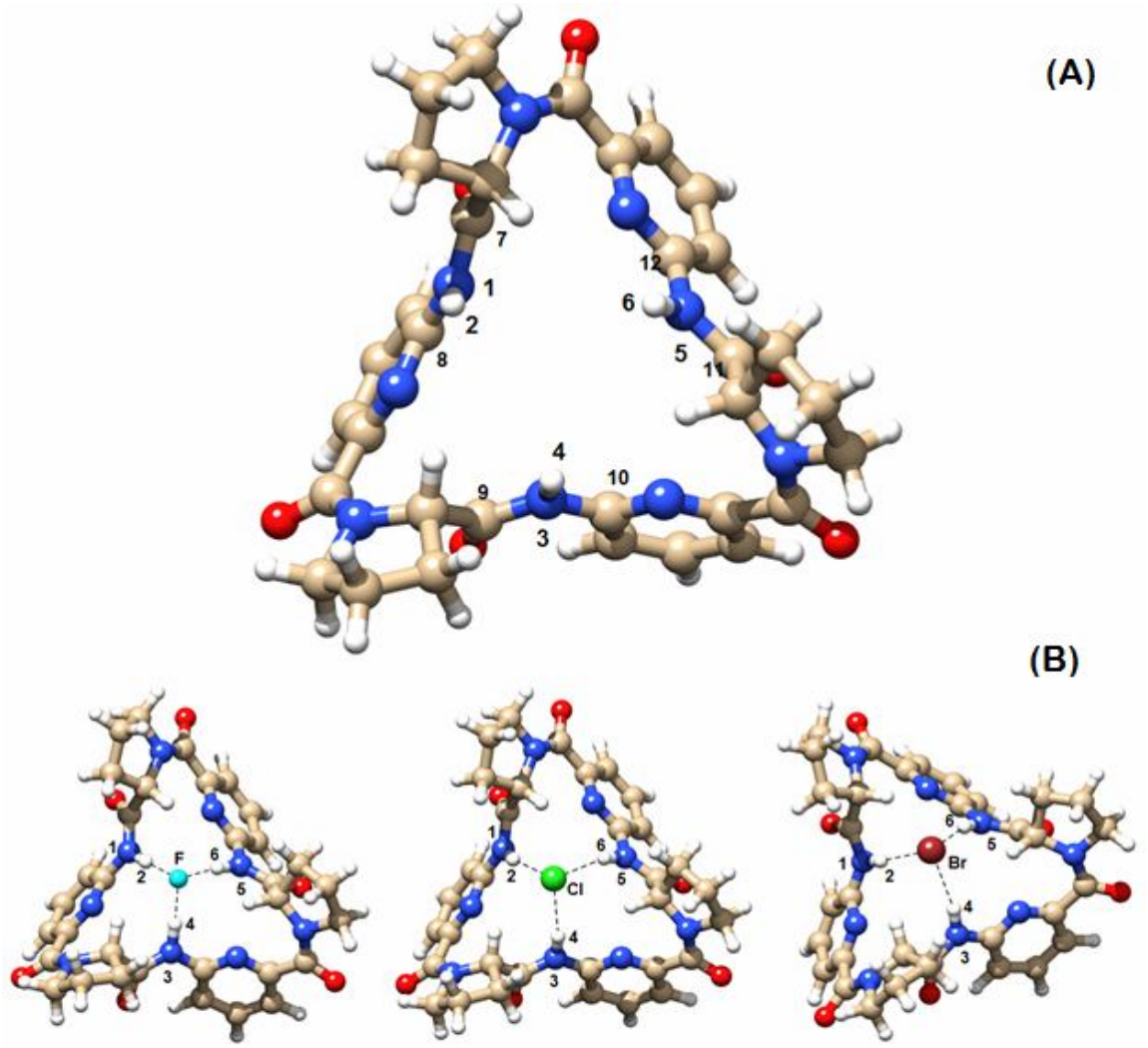

Fig. 1. Optimized structures of the (A) free CP and (B) CP-X complexes with atom numbering at the M05-2X/6-31G(d) level in the gas phase.

formation of the selective complexes with alkaline earth metal ions in the gas phase and water [33]. Our results indicated that CP composed of alanine makes the most stable complexes with these cations and all complexes are more stable in the gas phase than water.

In this article, we investigate the ability of the cyclic nano-hexapeptide consists of L-proline and 6-aminopicolinic acid for the selective extraction of halide ions such as F^-, Cl^-, Br^- and ion pairs including Na^+F^-, Na^+Cl^- and Na^+Br^- in the gas phase. To have a better insight into the interaction of this CP and halide ions, dispersion corrected density functional theory (DFT-D3) calculations is used and the dispersion energies during the complex formation are taken into account. Finally, natural bond orbital analysis and quantum theory of atoms in molecules (QTAIM) are performed on the complexes of the CP and halide ions. The importance of this study is to predict the selective extraction power of the CP against to halide ions and the corresponding ion pairs.

COMPUTATIONAL METHODS

The structures of the free cyclic nano-hexapeptide, the complexes of the CP with halides (CP-X (X = F^-, Cl^- and Br^-)) and

ion pairs (Na-CP-X) were optimized in the gas phase by M05-2X [34,35] and M05-2X-D3 [36,37] functionals, using the 6-31G(d) basis set [38]. To eliminate the effect of the basis set incompleteness, E_{BSSE} as the basis set superposition error (BSSE) correction was calculated by employing the counterpoise correction method. To provide an estimation of the zero-point vibrational energies (ZPVEs) as well as the corresponding thermochemical parameters of the CP complexes, frequency calculations were performed. The energy difference obtained by these functionals is a scale of the dispersion interaction energies.

To study the charge transfer and donor-acceptor interaction energies during the complex formation, NBO analysis was performed [39]. All the calculations were carried out using the Gaussian 09 package [40]. The electron localization function (ELF) [41-48], localized orbital locator (LOL) [48,50] and QTAIM [49] analyses were applied by MultiWFN 3.1 [51] to describe the interaction between the CP, ions and ion pairs.

RESULTS AND DISCUSSION

Structural Analysis

The optimized structure of the CP containing L-proline and 6-aminopicolinic acid is presented in Fig. 1. X-ray crystallography analysis of this CP [52] shows that the conformation of the peptide in the crystal has exact C3 symmetry and the calculation was performed accordingly. In Fig. 1, all N-H and C=O groups are transoid and all the N-H groups are arranged on the same side as the nitrogen atoms of the pyridine rings.

Main geometrical parameters of the free CP and CP-X complexes in the gas phase are reported in Table 1. The calculated average bond length of C=O and C-N by M05-2X-D3 are 1.23 and 1.36 Å, respectively, which are in agreement with the experimental data [52]. The experimental average bond length of C=O and C-N are 1.23 and 1.36 Å, respectively. Moreover, the average angle of CNH of the free CP is 118.06˚, in accordance to the experimental value of 117.70˚. These results indicate that for the current purpose, the results derived from the M05-2X and M05-2X-D3/6-31G(d) levels will suffice.

The optimized structures of the CP-X complexes in Fig. 1, show that all halide ions (X^-) have three hydrogen bonds (H-bond) with the N-H groups of the CP. The comparison of the free CP and CP-X complexes indicate that during the H-bond formation N-H bond length increases, the N-H bond length of the free CP is 1.01 Å while for the complexes with F^-, Cl^- and Br^- is 1.05, 1.02 and 1.02 Å, respectively. The calculated $H^{\cdots}X^-$ distance by the M05-2X and M05-2X-D3 functionals is as follows: $H^{\cdots}Br^- > H^{\cdots}Cl^- > H^{\cdots}F^-$. Therefore, F^- has the strongest H-bond with the CP, because of the reverse correlation of the $H^{\cdots}X^-$ bond length and the interaction energy.

The ability of the CP to form the selective complexes with the ion pairs such as Na^+F^-, Na^+Cl^- and Na^+Br^- were investigated in the gas phase. The optimized structures of the CP with ion pairs (Na-CP-X) are displayed in Fig. 2 and the selected geometrical parameters are provided in Table 2. According to Table 2, in the Na-CP-X complexes halide anions have longer H-bond distance than the CP-X complexes. For example, the average $H^{\cdots}F^-$ bond length of the CP-X and Na-CP-X are 1.62 and 1.84 Å, respectively.

An insight into the bond lengths indicates that an increase in the halide ion size has not important effect on the distance of the Na^+-N. Moreover, Na-X bond lengths in the NaCPX complexes are bigger than those in free Na-X bond length. The calculated Na-X bond length, of the free NaF, NaCl and NaBr, at the M05-2X level, are 1.88, 2.38 and 2.49 Å, respectively, while for the Na-CP-X complexes are 2.10, 2.57 and 2.69 Å, respectively. Calculated IR vibrational frequencies of the $H^{\cdots}Br^-$, $H^{\cdots}Cl^-$ and $H^{\cdots}F^-$ bonds at the M05-2X level of the theory of the CPX complexes are 3379.23, 3360.32 and 3087.34 cm^{-1}, respectively, while the calculated frequencies of these bonds are 3451.63, 3460.21 and 3332.16 cm^{-1} for the NaCPX complexes.

Energy Analysis

Binding energy (ΔE_{bin}) is obtained according to the Eqs. (1) and (2), where E_{comp} is the energy of the complexes, E_{CP} is the energy of the cyclic peptide, E_{BSSE} is the basis set superposition error (BSSE), and E_X and E_{Na+X}^- are the energies of the halide ions and ion pairs, respectively.

$$\Delta E_{bin} = E_{Comp} - E_{CP} - E_X^- + E_{BSSE} \quad (1)$$

$$\Delta E_{bin} = E_{Comp} - E_{Na+X}^- - E_{CP} + E_{BSSE} \quad (2)$$

ΔE_{bin} values of the CP-X and NaCPX complexes are reported in Table 3. In the case of the CP-X structures, the stability of the complexes is as follows:

$CP\text{-}F^- > CP\text{-}Cl^- > CP\text{-}Br^-$

Table 1. Main Geometrical Parameters of the Free CP and CP-X Complexes by M05-2X and M05-2X-D3 in the Gas Phase (Bond Lengths and Angles are in Å and Degrees, Respectively)

	M05-2X				M05-2X-D3				
Bond	CP	F^-	Cl^-	Br^-	CP	F^-	Cl^-	Br^-	X-ray
N1H1	1.008	1.050	1.025	1.023	1.008	1.049	1.025	1.024	0.860
N3H4	1.009	1.049	1.025	1.023	1.008	1.049	1.025	1.024	0.860
N5H6	1.009	1.049	1.025	1.023	1.008	1.049	1.025	1.024	0.860
$H2X^-$	-	1.624	2.316	2.429	-	1.623	2.314	2.427	-
$H4X^-$	-	1.625	2.316	2.429	-	1.623	2.317	2.425	-
$H6X^-$	-	1.624	2.316	2.429	-	1.622	2.315	2.426	-
C7N1H2	118.08	120.03	118.21	118.23	118.04	120.10	118.38	118.23	117.69
C9N3H4	118.00	120.05	118.21	118.17	118.03	120.10	118.37	118.23	117.64
C11N5H6	118.00	120.03	118.27	118.15	118.01	120.10	118.35	118.18	117.74

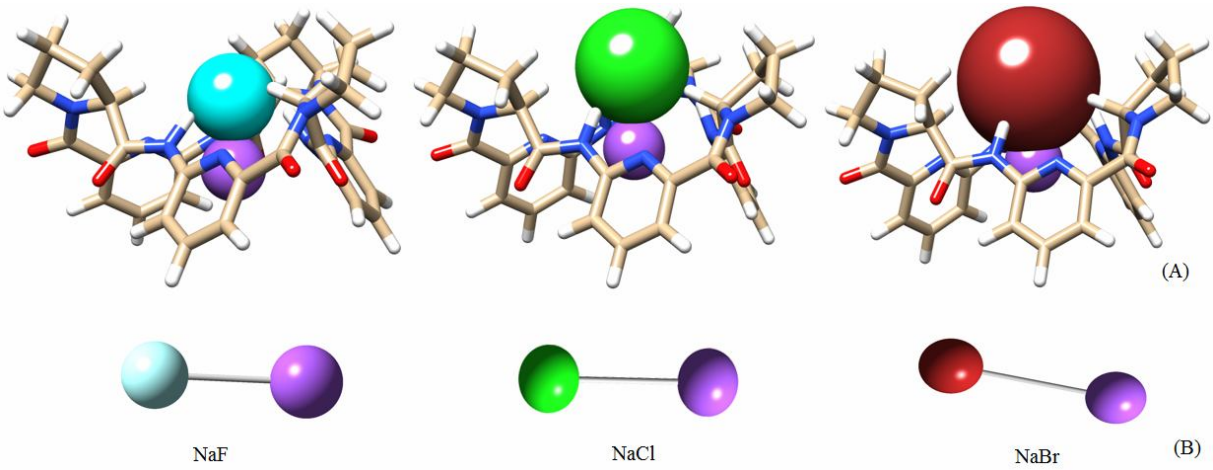

Fig. 2. The Optimized structures of the (A) NaCPX complexes and (B) free NaX in the gas phase at the M05-2X level.

This trend is in contrast to the ionic radii. Since the electronegativity and electron density [53] of the F^- are more than those of Br^- and Cl^-, therefore the CP-F^- complex is more stable than other CP-X complexes due to the stronger H-bond formation between the CP and F^- ion. According to Table 3, NaCPX complexes are more stable than CP-X complexes.

Comparison between the ΔE of the NaCPX and CP-X indicate that this CP is a good receptor in the selective ion pair complex formation. According to Table 3, the stability of the CP-ion pair complexes is as follows:

$$Na^+CPF^- > Na^+CPCl^- > Na^+CPBr^-$$

Table 2. Selected Geometrical Parameters of the Na-CP-X Complexes in the Gas Phase at the M05-2X and M05-2X-D3 Levels (Bond Length is in Å)

	M05-2X			M05-2X-D3		
Bond	F^-	Cl^-	Br^-	F^-	Cl^-	Br^-
N1H2	1.031	1.021	1.021	1.030	1.021	1.021
N3H4	1.030	1.021	1.021	1.031	1.021	1.021
N5H6	1.030	1.021	1.021	1.031	1.021	1.021
$H2X^-$	1.836	2.514	2.566	1.834	2.512	2.567
$H4X^-$	1.833	2.512	2.566	1.836	2.510	2.567
$H6X^-$	1.837	2.512	2.567	1.836	2.513	2.567
NaX	2.102	2.574	2.689	2.104	2.575	2.690
Na^+N1	2.557	2.565	2.590	2.558	2.555	2.582
Na^+N3	2.556	2.565	2.591	2.550	2.557	2.583
Na^+N5	2.557	2.567	2.592	2.552	2.557	2.583

Table 3. Thermodynamic Parameters (kcal mol^{-1}) of the Complex Formation in the Gas Phase

	M05-2X			M05-2X-D3		
Structures	ΔE_{bin}	ΔH_{bin}	ΔG_{bin}	ΔE_{bin}	ΔH_{bin}	ΔG_{bin}
CP-F^-	-85.18	-126.69	-117.19	-86.69	-127.79	-118.63
CP-Cl^-	-57.69	-65.26	-56.78	-58.60	-66.30	-57.73
CP-Br^-	-52.97	-73.70	-64.98	-54.16	-74.90	-65.85
Na-CP-F	-198.92	-251.07	-234.14	-199.66	-251.81	-234.66
Na-CP-Cl	-171.00	-185.43	-169.13	-172.26	-186.70	-170.01
Na-CP-Br	-165.84	-196.61	-180.04	-167.23	-197.63	-181.12

This trend is in accordance to the obtained results for the CP-X complexes. Binding enthalpy (ΔH_{bin}) and binding Gibbs free energies (ΔG_{bin}) of the CP complex formation reaction were calculated and reported in Table 3, too.

According to ΔH_{bin} values, the formation of the halide ions and ion pair complexes are exothermic according to $F^- > Br^- > Cl^-$ trend for both of the CP-X and NaCPX complexes. Moreover, ΔG_{bin} values show that ion and ion pair complex formation are thermodynamically favorable and the complexes have a good stability in the gas phase.

To have a better insight into the interaction of the ion, ion pair and CP, density functional theory dispersion correction was used

Table 4. Calculated Dispersion Energies (kcal mol^{-1}) of the Complex Formation

	Ion			Ion pair		
Structures	ΔE_{dis}	ΔH_{dis}	ΔG_{dis}	ΔE_{dis}	ΔH_{dis}	ΔG_{dis}
F^-	-1.51	-1.10	-1.44	-0.74	-0.74	-0.52
Cl^-	-0.91	-1.04	-0.95	-1.26	-1.27	-0.88
Br^-	-1.19	-1.20	-0.87	-1.39	-1.02	-1.08

Table 5. Calculated E(2) Values (kcal mol^{-1}) of the CP Complexes in the Gas Phase at the M05-2X/6-31G(d) Level

	Ion complex (CP-X)				
	σ^*_{N1-H2}	σ^*_{N3-H4}	σ^*_{N5-H6}	$\sum E(2)$	Lp^*_{Na+}
Lp_{F-}	44.20	45.69	44.24	134.12	-
Lp_{Cl-}	17.02	17.05	17.02	51.09	-
Lp_{Br-}	17.48	17.83	17.44	52.75	-
	Ion pair complex (NaCPX)				
Lp_{F-}	19.21	19.30	19.23	57.05	19.05
Lp_{Cl-}	6.04	6.08	6.05	18.17	65.63
Lp_{Br-}	7.02	7.17	7.19	21.38	95.19

Table 6. Selected Atomic Charges of the CP Complexes

	Ion complex				Ion pair complex		
Atoms	CP	F^-	Cl^-	Br^-	F^-	Cl^-	Br^-
H2	0.435	0.483	0.467	0.458	0.473	0.466	0.461
H4	0.435	0.483	0.467	0.458	0.473	0.466	0.461
H6	0.434	0.483	0.467	0.458	0.474	0.466	0.461
N1	-0.653	-0.685	-0.665	-0.665	-0.730	-0.721	-0.721
N3	-0.653	-0.685	-0.665	-0.665	-0.730	-0.721	-0.721
N5	-0.653	-0.685	-0.665	-0.665	-0.729	-0.720	-0.721
X^-	-1.000	-0.734	-0.664	-0.816	-0.795	-0.827	-0.778
Na^+	1.000	-	-	-	0.822	0.745	0.719

for calculating the dispersion interaction energies between these structures. According to Table 3, all the thermodynamic parameters computed by the M05-2X-D3 functional are more than those obtained by the M05-2X one. Therefore, the obtained differences by these functionals can be considered as the complex dispersion interaction energies which are reported in Table 4.

According to Table 4, the dispersion interaction energies of the complexes are small and with increasing the size of the halide ions binding dispersion energy (ΔE_{dis}) is elevated. Na-CP-F complex has the minimum dispersion interaction, while Na-CP-Br has the maximum value. A small value of the dispersion energy reveals that dispersion interaction is not very important for the complex formation while the electrostatic interaction between the ions and CP is the driving force for the complex formation. Therefore, because of the small size of the fluoride, the electrostatic interaction in the CP-F^- complex formation is more important than dispersion interaction.

Charge Transfer and Quantum Reactivity Indices

To study the charge transfer and orbital interaction, during the complex formation between the ions and CP, NBO analysis has been performed. The perturbation stabilization energies, E(2), obtained by the NBO analysis are reported in Table 5. A complex with a higher value of E(2) is more stable in comparison to a complex with a small value of the stabilization energy.

For the host-guest complexes, the maximum interactions are between lone pair electrons of X^- (donor) and σ* orbital of N-H bonds (acceptor) of the CP. According to Table 5, the calculated E(2) energies of the CP-X complexes between the Lp_{X-} and σ^*_{N-H} reveals that F^- has the most interaction in comparison to other halides. Moreover, E(2) values of the CP-X complexes are as follows: $F^- > Br^- > Cl^-$, which is in a geed agreement with the results of the energy analysis. This indicates that CP-F^- and CP-Br^- are more stable complexes than CP-Cl^- due to more efficient orbital interaction between the ions (guest) and the CP (host). E(2) values of ion pair complexes are smaller than the E(2) values of the CP-X complexes and show that during the ion pair complex formation, interactions between the Lp_{X-} and σ^*_{N-H} orbitals have been reduced.

The stability of the ion pair complexes are in accordance to $F^- > Br^- > Cl^-$, similar to the trend of the CP-X complexes. The interaction of Lp_{Br-} and Lp^*_{Na+} has the most E(2) value (95.19 $kcal.mol^{-1}$) which is sufficient for the Na^+Br^- bond formation of the ion pair complex. These results indicate that electrostatic interactions between Lp_{X-} and σ^*_{N-H} of the CP is the driving force for the complex formation.

Atomic charge analysis (Table 6) shows that the positive and negative charges of the H and N atoms, respectively, increased during the complex formation in comparison to the free CP while a negative charge reduction is observed for the halide ions (X^-) and Na^+. These changes of the atomic charges indicate a charge transfer from the halide to Na^+ during the ion pair complex formation.

For investigation of the reactivity of the free CP and complexes, HOMO-LUMO analysis was performed. A pictorial presentation of the frontier orbitals is provided in Fig. 3. According to Fig. 3, HOMOs are localized partly on the halide of the CP-X structures while the LUMOs are on the CP structure. Moreover, in the NaCPX complexes, HOMO and LUMO orbitals were investigated in the cyclic peptide structure. Based on this analysis, quantum chemistry reactivity indices [54] such as HOMO energy (E_{HOMO}), LUMO energy (E_{LUMO}), electronic chemical potential (μ), chemical hardness (η) and electrophilicity index (ω) have calculated and reported in Table 7.

According to Table 7, during the complex formation, η value is reduced and the calculated values of the η show that the order of reactivity of the CP-X and NaCPX complexes are according to: $Br^- > F^- > Cl^-$ and $F^- > Br^- > Cl^-$, respectively. The chemical potential of the CP-X complexes increased in comparison to the free CP while the calculated μ of the ion pair complexes show the opposite behavior. Moreover, CP-X complex formation reduces the electrophilicity index, while ion pair complex formation increases the ω in comparison to the free CP.

QTAIM, LOL, ELF and Bond Order Analyses

By using the QTAIM analysis, some topological parameters such as electron density (ρ), Laplacian ($\nabla^2\rho$), kinetic energy density (G), potential energy density (V) and bond order (BO) were calculated at the bond critical points (BCP) between the ions and CP, and reported in Table 8. According to Table 8, the average values of the electron density of the $F^{-}\cdots H$, $Cl^{-}\cdots H$ and $Br^{-}\cdots H$ bonds of the CP-X complexes are 0.052, 0.021 and 0.020, respectively. This indicates that F^- has the strongest interaction with the CP in comparison to other ions.

Electron density values of the ion pair complexes show similar results and reveals that the Na^+F^- ion pair has the most interaction with the CP. Calculated $\nabla^2\rho$ values of the ion and ion pair complexes, Table 8, are positive and indicate an electrostatic

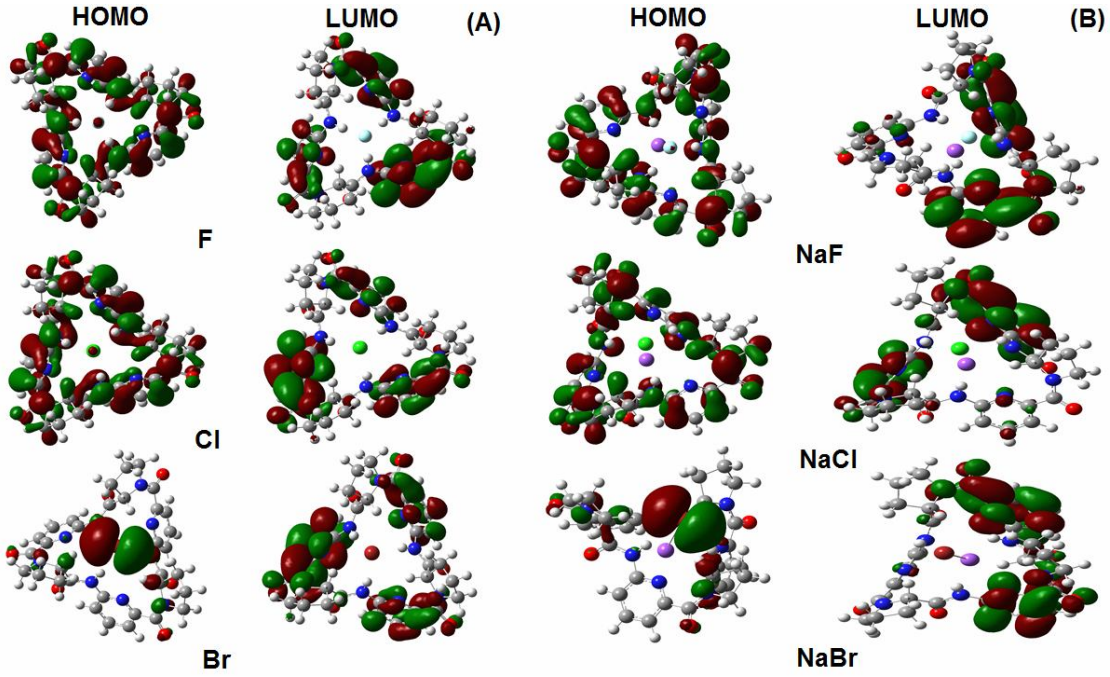

Fig. 3. Frontier molecular orbital diagrams of (A) CP-X and (B) ion pair complexes.

Table 7. Calculated Values of Electronic Chemical Potential, Chemical Hardness, Electrophilicity Index and HOMO-LUMO Orbital Energies (a.u.) of the CP and Ion Complexes

Structures	E_{HOMO}	E_{LUMO}	μ	η	$10^3\omega$
		Ion complex			
CP	-0.288	-0.009	-0.148	0.279	39.25
F^-	-0.186	0.085	-0.055	0.271	5.58
Cl^-	-0.191	0.081	-0.055	0.272	5.56
Br^-	-0.188	0.080	-0.054	0.268	5.44
		Ion pair complex			
F^-	-0.298	-0.024	-0.161	0.274	47.30
Cl^-	-0.302	-0.025	-0.164	0.277	48.25
Br^-	-0.301	-0.025	-0.163	0.276	48.13

interaction between the X^- ions and H atoms of the CP. The ratio of the kinetic energy density to the potential energy density (-G/V) at the BCP is a useful parameter for determination of the interaction class. According to Table 8, the average values of -G/V of the $F^-\cdots H$, $Cl^-\cdots H$ and $Br^-\cdots H$ bonds of the CP-X complexes are 0.88, 0.98 and 0.99, respectively, which reveal a

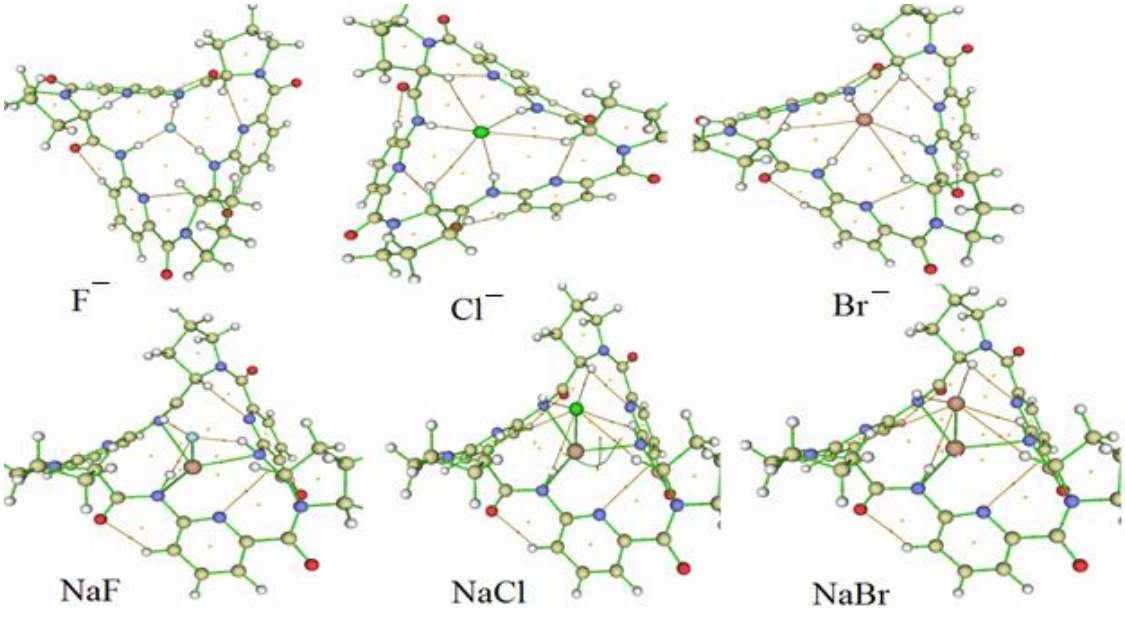

Fig. 4. Molecular graphs of the ion and ion pair complexes.

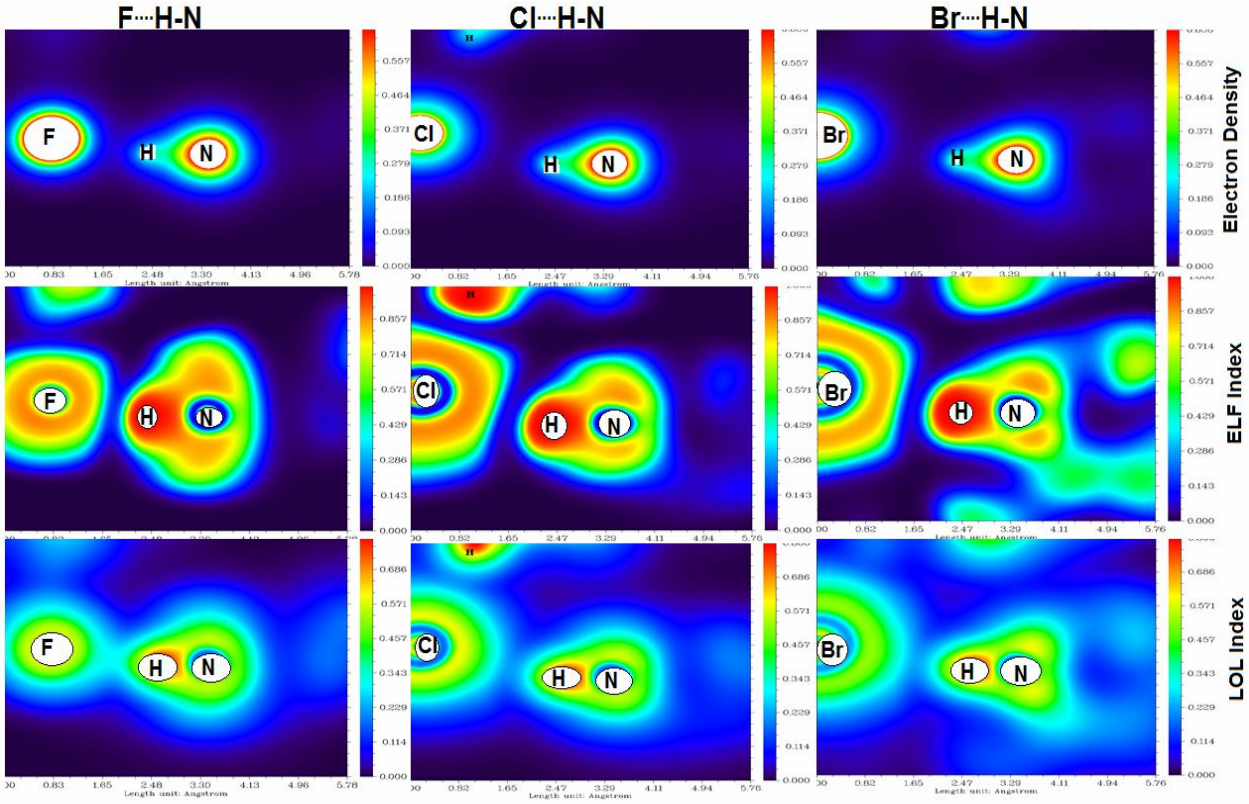

Fig. 5. Electron density, ELF and LOL diagrams of the halide ion complexes.

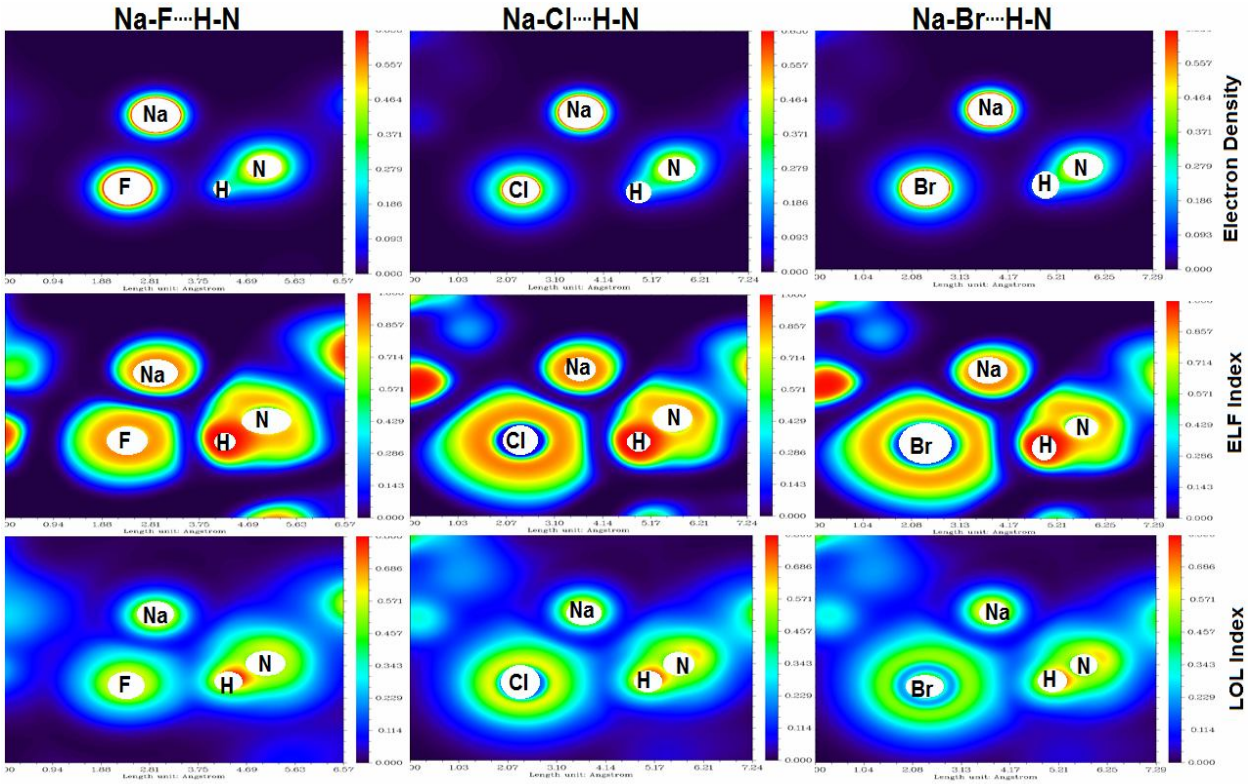

Fig. 6. Electron density, ELF and LOL diagrams of the ion pair complexes.

Table 8. Calculated Topological Parameters at the BCP of the $X^{-}\cdots H$ Bonds of the Ion and Ion Pair Complexes

Parameters	$F^{-}\cdots H2$	$F^{-}\cdots H4$	$F^{-}\cdots H6$	$Cl^{-}\cdots H2$	$Cl^{-}\cdots H4$	$Cl^{-}\cdots H6$	$Br^{-}\cdots H2$	$Br^{-}\cdots H4$	$Br^{-}\cdots H6$
Ion complex									
ρ	0.052	0.052	0.052	0.021	0.021	0.021	0.020	0.020	0.020
$\nabla^2\rho$	0.163	0.163	0.163	0.061	0.061	0.061	0.053	0.053	0.053
-G/V	0.886	0.886	0.886	0.987	0.987	0.987	0.992	0.992	0.993
BO	0.120	0.120	0.120	0.083	0.084	0.083	0.089	0.090	0.090
Ion pair complex									
ρ	0.032	0.033	0.033	0.015	0.015	0.015	0.016	0.016	0.016
$\nabla^2\rho$	0.110	0.110	0.110	0.049	0.049	0.049	0.048	0.048	0.048
-G/V	0.907	0.910	0.908	1.112	1.112	1.112	1.088	1.088	1.088
BO	0.067	0.067	0.067	0.041	0.041	0.041	0.060	0.060	0.060

partially covalent interaction between the halide and H atoms of the CP.

The calculated ratio of -G/V for $Cl^-\cdots H$ and $Br^-\cdots H$ in the ion pair complexes are more than 1.0 and shows a non-covalent interaction between the ion pair and CP. The values of the BO indicate that F^- ion and the Na^+F^- ion pair have the most interaction with CP, too. These results indicate that halides have stronger interaction in comparison to the ion pair with CP.

To have an insight into the interaction between the ion and ion pair with the CP, the molecular graphs of the complexes are presented in Fig. 4. This figure illustrates the bond formation and interaction between the ions and ion pairs with the CP. ELF and LOL analyses of the $X^-\cdots HN$ interaction were performed.

Figures 5 and 6, show the LOL, ELF and electron density diagrams of the interaction between the ions and CP. These figures indicate that the ELF and LOL values are small and reveal the electrostatic interaction between the ions and CP. Moreover, Figs. 5 and 6 indicate that F^- has stronger interaction with CP in comparison to other ions, in both of the ion and ion pair complexes, with larger values of the ELF and LOL, according to the previous results.

CONCLUSIONS

DFT and DFT-D3 calculations have been performed for investigation of the interaction between the halide ion and CP. The electrostatic interactions of the ions and CP is a driving force for the complex formation while the dispersion interactions are not important. Moreover, the obtained results indicated that an increase in the size of the halide increases the dispersion interaction energies.

CP-F^- and NaCPF complexes are the most stable complexes from the energy view point. Finally, QTAIM and NBO analyses confirmed the electrostatic interactions of the halide and CP. Moreover, these analyses indicate that F^- makes the most stable complexes due to proper charge transfer, most orbital interaction and the strongest H-bond formation with the CP. Based on this study, the selective extraction power of the CP can be predicted for different halide ions and their ion pairs.

ACKNOWLEDGEMENTS

Research Council of Ferdowsi University of Mashhad is acknowledged for financial supports. We hereby acknowledge that part of this computation was performed on the HPC center of Ferdowsi University of Mashhad.

REFERENCES

[1] Steed, J. W.; Atwood, J. L., Supramolecular Chemistry, John Wiley & Sons Ltd., 2nd edition, 2010.

[2] Lehn, J. M., Supramolecular Chemistry: Concepts and Perspectives, VCH, Weinheim, Germany, 1995.

[3] Atwood, J. L.; Davies, J. E. D.; Nicol, D. D. M.; Vogtle, F.; Lehn, J. M., Supramolecular Chemistry, Pergamon, Oxford, UK., 1996.

[4] Bianchi, A.; Bowman-James, K.; Garcı´a-Espan˜a, E., Supramolecular Chemistry of Anions Wiley-VCH, New York, 1997.

[5] Sessler, J. L.; Gale, P. A.; Cho, W. S., Royal Society of Chemistry, Cambridge, UK., 2006.

[6] Wenzel, M.; Hiscock, J. R.; Gale, P. A., Anion receptor chemistry: highlights from 2010. Chem. Soc. Rev., 2012, 41, 480-520, DOI: 10.1039/C1CS15257B.

[7] Gale, P. A., Anion receptor chemistry. *Chem. Commun.,* **2011**, *47*, 82-86, DOI: 10.1039/C0CC00656D.

[8] Gale, P. A., Anion receptor chemistry: highlights from 2008 and 2009. *Chem. Soc. Rev.,* **2010**, *39*, 3746-3771, DOI: 10.1039/C001871F.

[9] Caltagirone, C.; Gale, P. A, Anion receptor chemistry: highlights from 2007. *Chem. Soc. Rev.,* **2008**, *38*, 520-563, DOI: 10.1039/B806422A.

[10] Gale, P. A.; Garcia-Garrido, S. E.; Carric, J., Anion receptors based on organic frameworks: highlights from 2005 and 2006. *Chem. Soc. Rev.,* **2008**, *37*, 151-190, DOI: 10.1039/B715825D.

[11] Katayev, E. A.; Ustynyuk, Y. A.; Sessler, J. L., Receptors for tetrahedral oxyanions. *Coord. Chem. Rev.,* **2006**, *250*, 3004-3037.

[12] Stern, K. H.; Amis, E. S., *Ionic Size. Chem. Rev.,* **1959**, *59*, 1-64, DOI: 10.1021/cr50025a001.

[13] Ravikumar, I.; Ghosh, P., Recognition and separation of sulfate anions. *Chem. Soc. Rev.,* **2012**, *41*, 3077-3098, DOI: 10.1039/C2CS15293B.

[14] Mateus, P.; Bernier, N.; Delgado, R., Recognition of anions by polyammonium macrocyclic and cryptand receptors: Influence of the dimensionality on the binding behavior. *Coord. Chem. Rev.,* **2010**, *254*, 1726-1747.

[15] Duncan, R.; Gaspar, R., Nanomedicine(s) under the Microscope. *Mol. Pharmaceutics.,* **2011**, *8*, 2101-2141, DOI: 10.1021/mp200394t.

[16] Lin, Y.; Taylor, S.; Li, H.; Fernando, K. A. S.; Qu, L.; Wang, W.; Gu, L.; Zhou, B.; Sun, Y. P., Advances toward bioapplications of carbon nanotubes. *J. Mater. Chem.* **2004**, *14*, 527-541, DOI: 10.1039/B314481J.

[17] Martin, C. R.; Kohli, P., The emerging field of nanotube biotechnology. *Nat. Rev. Drug. Discovery.* **2003**, *2*, 2937, DOI: 10.1038/nrd988.

[18] Chen, G. J.; Su, S.; R. Z. Liu, Theoretical Studies of Monomer and Dimer of Cyclo[(-l-Phe1-d-Ala2-)n] and Cyclo[(-l-Phe1-d-MeN-Ala2-)n] (n = 3-6*). J. Phys. Chem. B.,* **2002**, 16, 1570-1575, DOI: 10.1021/jp0114790.

[19] Teranishi, M.; Okamoto, H.; Takeda, K.; Nomura, K.; Nakano, A.; Kalia, R. K.; Vashishta Shimojo, P. F., Molecular dynamical approach to the conformational transition in peptide nanorings and nanotubes. *J. Phys. Chem. B.,* **2009**, *113*, 1473-1484, DOI: 10.1021/jp8067975.

[20] Hartgerink, J. D.; Granja, J. R.; Milligan, R. A.; Ghadiri, M. R., Self-Assembling Peptide Nanotubes. *J. Am. Chem. Soc.,* **1996**, *118*, 43-50, DOI: 10.1021/ja953070s.

[21] Tan, H. W.; Qu, W. W.; Chen, G. J.; Liu, R. Z., Theoretical investigation of the self-assembly of cyclo[(-β3-HGly)4-]. *Chem. Phys. Lett.,* **2003**, *369*, 556-561, DOI: 10.1016/S0009-2614(02)01372-6.

[22] Poteau, R.; Trinquier, G., All-cis cyclic peptides. *J. Am. Chem. Soc.,* **2005**, *127*, 13875-13889, DOI: 10.1021/ja052342g.

[23] Boyle, T. P.; Bremner, J. P.; Coates, J.; Deadman, J.; Keller, P. A., New cyclic peptides via ring-closing metathesis reactions and their anti-bacterial activities. *Tetrahedron* **2008**, *64*, 11270-11290, DOI: 10.1016/j.tet.2008.09.031.

[24] Cheng, L.; Naumann, T. A.; Horswill, A. R.; Hong, S. J.; Venters, B. J.; Tomsho, J. W.; Benkovic, S. J.; Keiler, K. C., Discovery of antibacterial cyclic peptides that inhibit the ClpXP protease. *Protein. Sci.,* **2007**, *16*, 1535-1542, DOI: 10.1110/ps.072933007.

[25] Femandez-Lopez, S.; Kim, H. S.; Choi, B. C.; Delgado, M.; Granja, J. R.; Khasanov, A.; Kraehenbuehl, K.; Long, G.; Weinberger, D. A.; Wilcoxen, K. M.; Ghadiri, M. R., Antibacterial agents based on the cyclic D,L-alpha-peptide architecture. *Nature.*, **2001**, *412*, 452-455, DOI: 10.1038/35086601.

[26] Matsumoto, T.; Nishimura, K.; Takeya, K., New Cyclic Peptides from Citrus medica var. sarcodactylis SWINGLE. *Chemical. Pharm. Bull.,* **2002**, *50*, 857-560, DOI: 10.1248/cpb.50.857.

[27] Maryanoff, B. E.; Greco, M. N.; Zhang, H. C.; Andrade-Gordon, P.; Kauffman, J. A.; Nicolaou, K. C.; Liu, A.; Brungs, P. H., Macrocyclic peptide inhibitors of serine proteases. Convergent total synthesis of cyclotheonamides A and B *via* a late-stage primary amine intermediate. Study of thrombin inhibition under diverse conditions. *J. Am. Chem. Soc.,* **1995**, *117*, 1225-1239, DOI: 10.1021/ja00109a006.

[28] Dahiya, R., Synthesis of a phenylalanine-rich peptide as potential anthelmintic and cytotoxic agent. *Acta. Pol. Pharm. Drug. Res.,* **2007**, *64*, 509-5016.

[29] Montengro, J.; Ghadiri, M. R.; Granja, J. R., Ion channel models based on self-assembling cyclic peptide nanotubes. *Acc. Chem. Res.,* **2013**, *46*, 29552965, DOI: 10.1021/ar400061d.

[30] Garcia-Fandino, R.; Amorin, M.; Castedo, L.; Granja, R., Transmembrane ion transport by self-assembling α,γ-peptide nanotubes. *Chem. Sci.,* **2012**, *3*, 3280-3285, DOI: 10.1039/C2SC21068A.

[31] Jafari Chemahini, Z.; Najafi Chermahini, A.; Dabbagh, H. A.; Teimouri, A., Complexation of all-cis cyclo(L-Pro)3 and alkali metal cations: a DFT study. *J. Incl. Phenom. Macrocycl. Chem.,* **2015**, *81*, 465-473, DOI: 10.1007/s10847-015-0476-0.

[32] Najafi Chermahini, A.; Rezapour, M.; Teimouri, A., Selective complexation of alkali metal ions and nanotubular cyclopeptides: a DFT study. *J. Incl. Phenom. Macrocycl. Chem.,* **2014**, *79*, 205-214, DOI: 10.1007/s10847-013-0346-6.

[33] Khavani, M.; Izadyar, M.; Housaindokht, M. R., DFT investigation and molecular dynamic simulation on the selectivecomplexation of cis-cyclic nanopeptides with alkaline earth metalions. *Sensor. Actuat B. Chem.,* **2015**, *221*, 1120-1129, DOI; 10.1016/j.snb.2015.07.090.

[34] Zhao, Y.; Truhlar, D. G., A new local density functional for main-group thermochemistry, transition metal bonding, thermochemical kinetics, and noncovalent interactions. *J. Chem. Phys.* **2006**, *125*, 194101-194121, DOI: 10.1063/1.2370993.

[35] Zhao, Y.; Truhlar, D. G., Comparative DFT study of van der

Waals complexes: rare-gas dimers, alkaline-earth dimers, zinc dimer, and zinc-rare-gas dimers. *J. Phys. Chem. A.,* **2006**, *110*, 5121-5129, DOI: 10.1021/jp060231d.

[36] Grimme, S.; Ehrlich, S.; Goerigk, L., Effect of the damping function in dispersion corrected density functional theory. *J. Comp. Chem.,* **2011**, *32*, 1456-1465, DOI: 10.1002/jcc.21759.

[37] Grimme, S.; Antony, J.; Ehrlich, S.; Krieg, H., A consistent and accurate ab initio parametrization of density functional dispersion correction (DFT-D) for the 94 elements H-Pu. *J. Chem. Phys.,* **2010**, *132*, 154104-154124, DOI: 10.1063/1.3382344.

[38] Hohenberg, P.; Kohn, W., Inhomogeneous electron gas. *Phys. Rev. B.,* **1964**, *136*, 864-871.

[39] Reed, A. E.; Curtiss, L. A.; Weinhold, F., Intermolecular interactions from a natural bond orbital, donor-acceptor viewpoint. *Chem. Rev.,* **1988**, *88*, 899-926, DOI: 10.1021/cr00088a005.

[40] Frisch, J.; Trucks, G. W.; Schlegel, H. B.; Scuseria, G. E.; Robb, M. A.; Cheeseman, J. R.; Montgomery, J. A.; Vreven, T.; Kudin, K. N.; Burant, C. J.; *et al*., Gaussian 09; Gaussian, Inc.: Pittsburgh, P. A., 2009.

[41] Scherer, W.; Sirsch, P.; Shorokhov, D.; Tafipolsky, M.; GMcGrady. S.; E. Gullo, Valence charge concentrations, electron delocalization and β-agostic bonding in d0 metal alkyl complexes. *Chem. Eur. J*., **2003**, *9*, 6057-6070, DOI: 10.1002/chem.200304909.

[42] Shurki, A.; Hiberty, P. C.; Shaik, S., Charge-shift bonding in group IVB halides: A valence bond study of MH_3-Cl (M = C, Si, Ge, Sn, Pb) molecules. *J. Am. Chem. Soc.,* **1999**, *121*, 9768-9768, DOI: 10.1021/ja995530d.

[43] Becke, A. D.; Edgecombe, K. E., A simple measure of electron localization in atomic and molecular systems. *J. Chem. Phys.,* 1990, 92, 5397-5403, DOI: 10.1063/1.458517.

[44] Savin, A.; Nesper, R.; Wengert, S.; Fassler, T., ELF: The electron localization function. *Angew. Chem. Int. Ed. Engl.,* **1997**, *36*, 1808-1832, DOI: 10.1002/anie.199718081.

[45] Burdett, J. K.; McCormick, T. A., Electron localization in molecules and solids: the meaning of ELF. *J. Phys. Chem. A.,* **1998**, *102*, 6366-6372, DOI: 10.1021/jp9820774.

[46] Savin, A.; Jepsen, O.; Flad, J.; Andersen, O. K.; Preuss, H.; Schnering, H. G., Electron Localization in Solid-state Structures of the Elements: the Diamond Structure. *Angew. Chem. Int. Ed. Engl*., **1992**, *31*, 187-188, DOI: 10.1002/anie.199201871.

[47] Tsirelson, V.; Stash, A., Determination of the electron localization function from electron density. *Chem. Phys. Lett.,* **2002**, *351*, 142-148, DOI: 10.1016/S0009-2614(01)01361-6.

[48] Schmider, H. L.; Becke, A. D., Chemical content of the kinetic energy density. *J. Mol. Struct. (Theochem).,* **2000**, *527*, 51-61, DOI: 10.1016/S0166-1280(00)00477-2.

[49] Jacobsen, H., Localized-orbital locator (LOL) profiles of chemical bonding. *Can. J. Chem.,* **2008**, *86*, 695-702, DOI: 10.1139/v08-052.

[50] Bader, R. F. W., Oxford University Press: Oxford, 1990.

[51] Lu, T.; Chen, F. W., Multiwfn: A multifunctional wavefunction analyzer. *J. Comput. Chem.,* **2012**, *33*, 580-592, DOI: 10.1002/jcc.22885.

[52] Kubik, S.; Goddard, R.; Kichner, R.; Nolting, D.; Seidel, J., A Cyclic Hexapeptide Containing L-Proline and 6-Aminopicolinic Acid Subunits Binds Anions in Water. *Angew. Chem. Int. Ed.,* **2001**, *40*, 2648-2651, DOI: 10.1002/jcc.22885.

[53] Xia, Y.; Wang, X.; Zhang, Y.; Luo, B.; Liu, Y., Computational investigation of a new ion-pair receptor for calix[4]pyrrole. *J. Mol. Moldel.,* **2012**, *18*, 2291-2299, DOI: 10.1007/s00894-011-1243-9

[54] Izadyar, M.; Gholizadeh, M.; Khavani, M.; Housaindokht, M. R., Quantum chemistry aspects of the solvent effects on 3,4-dimethyl-2,5-dihydrothiophen-1,1-dioxide pyrolysis reaction. *J. Phys. Chem. A.,* **2013**, *117*, 2427-2433, DOI: 10.1021/jp312746y.